Published in final edited form as:
Nature. 1998 November 5; 396(6706): 81–84. doi:10.1038/23954.

Type III $InsP_3$ receptor channel stays open in the presence of increased calcium

Robert E. Hagar[*], **Angela D. Burgstahler**[†], **Michael H. Nathanson**[†], and **Barbara E. Ehrlich**[‡]

[*] Department of Physiology, University of Connecticut Health Center, Farmington, Connecticut 06030, USA

[†] Department of Medicine and Cell Biology, Yale University, New Haven, Connecticut 06520, USA

[‡] Department of Pharmacology and Cellular and Molecular Physiology, Yale University, New Haven, Connecticut 06520, USA

Abstract

The inositol 1,4,5-trisphosphate receptor ($InsP_3R$) is the main calcium(Ca^{2+}) release channel in most tissues. Three isoforms have been identified[1–6], but only types I and II $InsP_3R$ have been characterized[7,8]. Here we examine the functional properties of the type III $InsP_3R$ because this receptor is restricted to the trigger zone from which Ca^{2+} waves originate[9–11] and it has distinctive $InsP_3$-binding properties[12,13]. We find that type III $InsP_3R$ forms Ca^{2+} channels with single-channel currents that are similar to those of type I $InsP_3R$; however, the open probability of type III $InsP_3R$ isoform increases monotonically with increased cytoplasmic Ca^{2+} concentration, whereas the type I isoform has a bell-shaped dependence on cytoplasmic Ca^{2+}. The properties of type III $InsP_3R$ provide positive feedback as Ca^{2+} is released; the lack of negative feedback allows complete Ca^{2+} release from intracellular stores. Thus, activation of type III $InsP_3R$ in cells that express only this isoform results in a single transient, but global, increase in the concentration of cytosolic Ca^{2+}. The bell-shaped Ca^{2+}-dependence curve of type I $InsP_3R$ is ideal for supporting Ca^{2+} oscillations, whereas the properties of type III $InsP_3R$ are better suited to signal initiation.

When homogenates from RIN-5F cells, rat hepatocytes, and canine cerebellum were probed by western blot analysis with isoform-specific antibodies, RIN-5F cells contained no detectable type I $InsP_3R$ (Fig. 1a, lane 4) but did express type III $InsP_3R$ (Fig. 1b, lane 4). In contrast, both hepatocytes and cerebellum expressed type I $InsP_3R$ (Fig. 1a, lanes 1 and 3), but no detectable type III $InsP_3R$ (Fig. 1b, lanes 1 and 3). Thus, the $InsP_3R$ of RIN-5F cells is almost entirely the type III isoform, consistent with previous reports[14]. Immunocytochemistry demonstrated that type III $InsP_3R$ was diffusely distributed (Fig. 1c) and confirmed that type I $InsP_3R$ expression was minimal (Fig. 1d, e). These findings do not support a previous prediction that type III $InsP_3R$ is preferentially localized near the plasma membrane[15].

To test whether type III $InsP_3R$ forms a Ca^{2+} channel, we incorporated endoplasmic reticulum vesicles from cultured RIN-5F cells into planar lipid bilayers. Single-channel currents were observed through type III $InsP_3R$. Like type I $InsP_3R$, type III $InsP_3R$ required $InsP_3$ to open (Fig. 2a: compare top three and bottom three traces). The single-channel current of type III $InsP_3R$ measured at 0 mV with 55 mM Ba^{2+} on the lumenal side of the channel was ~2.5 pA, which is similar to that of type I $InsP_3R$ (ref. 7). The conductances of type III $InsP_3R$ (88 ± 4 pS; Fig. 2b) and type I $InsP_3R$ (85 ± 3 pS)[7] were also similar.

Corresondence and requests for materials should be addressed to R.E.H. at Department of Pharmacology, Yale University, 333 Cedar Street, New Haven, Connecticut 06520-8066, USA (rob@hermen.med.yale.edu).

A central feature of type I $InsP_3R$ is that Ca^{2+} acts as an allosteric regulator when $InsP_3$ is present. Maximum channel activity occurs when the concentration of free Ca^{2+} is 250 nM; there is a sharp decline in channel activity on either side of the maximum, with complete inhibition when cytosolic Ca^{2+} exceeds 5 μM (Fig. 3b, circles)[16,17]. This bell-shaped regulation provides amplification of the initial $InsP_3$ signal, as well as negative-feedback inhibition of further $InsP_3$-stimulated Ca^{2+} release. The feedback inhibition is particularly important because it provides autoregulation and is essential for Ca^{2+} oscillations and for the propagation of regenerative intracellular Ca^{2+} waves[18].

Does Ca^{2+} regulate type III $InsP_3R$ in the same way? We hypothesized that type III $InsP_3R$ should remain open at high cytoplasmic Ca^{2+} concentration ($[Ca^{2+}]$) because $InsP_3$ binding to type III $InsP_3R$ is not inhibited by elevated Ca^{2+} (refs 12, 13). To test this idea, we altered the cytoplasmic $[Ca^{2+}]$ in the presence of a fixed $InsP_3$ concentration (2 μM). Like type I $InsP_3R$, type III $InsP_3R$ was progressively activated as the cytoplasmic $[Ca^{2+}]$ increased to 250 nM. However, channel activity for type III $InsP_3R$ remained high even when cytoplasmic $[Ca^{2+}]$ was raised to 100 μM (Fig. 3a, bottom traces; Fig. 3b, triangles). The mean open time for type III $InsP_3R$ (6.5 ± 0.62 ms) was nearly identical to the reported value for type I $InsP_3R$ (6.4 ± 1.0 ms)[7] and was independent of the cytoplasmic Ca^{2+} concentration. Thus, cytoplasmic free Ca^{2+} regulates the two isoforms differently; although both isoforms show similar Ca^{2+}-dependent activation, Ca^{2+}-dependent inhibition is lacking for type III $InsP_3R$.

To investigate the physiological importance of this pattern of activation in an intact cell, we monitored the cytoplasmic $[Ca^{2+}]$ in RIN-5F cells which we stimulated with extracellular ATP that binds to P_{2Y} receptors and increases $[Ca^{2+}]$ through the $InsP_3$ cascade[19,20]. RIN-5F cells responded to ATP stimulation with a single, transient increase in $[Ca^{2+}]$ (Fig. 4a). In single cells, stimulation with 100 μM ATP induced a 209 ± 24% increase in Fluo-3 fluorescence relative to baseline; this increase lasted for 15.2 ± 0.8 s (Table 1). The response was similar in Ca^{2+}-free medium (Table 1). Similar, but slightly smaller, increases in Fluo-3 fluorescence were seen in cells stimulated with 10 μM or 1 μM ATP. There was no increase in $[Ca^{2+}]$ in response to stimulation with 0.1 μM ATP (Fig. 4b), and neither sustained nor repetitive increases in $[Ca^{2+}]$ (that is, Ca^{2+} oscillations) were seen in any of the cells. In contrast, hepatocytes, which contain only types I and II $InsP_3R$, produced Ca^{2+} oscillations after stimulation with 1 μM ATP (Fig. 4c), as shown previously[21]. RIN-5F cells that were serially stimulated with 10 μM and then 100 μM ATP responded only to the initial exposure to 10 μM ATP ($n = 8$). In addition, thapsigargin (2 μM) had a minimal effect on intracellular $[Ca^{2+}]$ when RIN-5F cells were pretreated with ATP (Fig. 4d). This finding provides direct evidence that activation of type III $InsP_3R$ drains internal Ca^{2+} stores in RIN-5F cells. Furthermore, the magnitude of ATP-induced Ca^{2+} spikes is significantly greater in RIN-5F cells than in hepatocytes (Fig. 4d, f). Thus, positive feedback of Ca^{2+} on type III $InsP_3R$ in RIN-5F cells causes rapid, massive, near-complete Ca^{2+} release, and results in more intense Ca^{2+} spikes that are of shorter duration than those that occur through the type I $InsP_3R$ in hepatocytes.

We next compared subcellular Ca^{2+} release from type III $InsP_3R$ in RIN-5F cells with subcellular Ca^{2+} release from type I $InsP_3R$ in SKHep1 cells (a hepatoma cell line that expresses type I but not type III $InsP_3R$; our unpublished observation). Small amounts of $InsP_3$ were released in both cell types by flash photolysis of microinjected caged $InsP_3$. Release of $InsP_3$ in the RIN-5F cells always resulted in all-or-none global Ca^{2+} signalling, although increases in $[Ca^{2+}]$ began in focal subcellular regions before spreading to encompass the entire cell (Fig. 5a–d). In contrast, non-propagating increases in $[Ca^{2+}]$ could sometimes be elicited in SKHep1 cells by photorelease of minimal amounts of $InsP_3$ (Fig. 5e–g, i), similar to responses previously seen in pancreatic acinar and HeLa cells and *Xenopus* oocytes[10,11,22,23]. Photorelease of larger amounts of $InsP_3$ induced a global Ca^{2+} response in SKHepI cells (Fig. 5h, j). These findings suggest that subcellular Ca^{2+} release via type III $InsP_3R$ results in

a positive-feedback cycle that leads to all-or-none Ca^{2+} signalling that spreads throughout the cell, whereas release through type I $InsP_3R$ with low concentratons of $InsP_3$ results in localized, non-propagating increases in $[Ca^{2+}]$.

The localized, subcellular Ca^{2+} signals in SKHep1 cells lasted from one to several seconds, a result that is typical for the duration of subcellular Ca^{2+} signals described in other mammalian cells[10,11,24]. Localized increases in $[Ca^{2+}]$ of shorter duration are routinely seen in *Xenopus* oocytes, in which Ca^{2+} puffs typically last for 300–1,000 ms (ref. 23). Although individual Ca^{2+} puffs are restricted to a small fraction of the total volume of an oocyte[23], they occupy a region that is larger than an entire mammalian cell. We believe that the localized elevation in $[Ca^{2+}]$ in SKHep1 cells is a reasonable mammalian cell equivalent of the localized Ca^{2+} signals described in oocytes.

Ca^{2+} concentrations in RIN-5F cells returned nearly to baseline after stimulation with ATP (Fig. 4a, d), although depletion of intracellular Ca^{2+} stores in other cells activates a robust store-operated Ca^{2+} current (I_{soc})[25]. Our findings suggest that I_{soc} is either small or absent in RIN-5F cells. We therefore stimulated RIN-5F cells with thapsigargin (2 μM) to deplete Ca^{2+} stores, and then removed Ca^{2+} from the medium. Thapsigargin induced a small but sustained increase in intracellular $[Ca^{2+}]$ (Fig. 4e); this increase was abolished by subsequent addition of extracellular EGTA. When RIN-5F cells were stimulated with thapsigargin in the absence of extracellular Ca^{2+}, there was no sustained increase in intracellular $[Ca^{2+}]$. Addition of thapsigargin to hepatocytes, in which I_{soc} has been described[25], induced a larger increase in intracellular $[Ca^{2+}]$ (Fig. 4g); the level of Ca^{2+} also returned to baseline in response to extracellular EGTA. These findings indicate that RIN-5F cells contain less I_{soc} than hepatocytes, which is interesting in light of a suggestion that the primary role of type III $InsP_3R$ is to initiate I_{soc} (ref. 15) rather than Ca^{2+} transients. This hypothesis was based upon heterologous expression studies in *Xenopus* oocytes in which the protein seems to be targeted to the cell surface and may differ from the distribution found in RIN-5F cells (Fig. 1b) and other mammalian cells[5,9].

The high degree of homology among $InsP_3R$ isoforms indicates that many of their functional properties ought to be comparable. We found that properties such as activation by $InsP_3$, the magnitude of the single-channel current, and activation by concentrations of Ca^{2+} less than 250 nM were quite similar. In addition, the sustained activity of type III $InsP_3R$ at raised Ca^{2+} concentrations is similar to that reported for type I $InsP_3R$ in the presence of high concentrations of $InsP_3$ (180 μM)[17]. In both cases, there is a lack of Ca^{2+}-dependent inhibition, and the channel remains open even when the cytoplasmic Ca^{2+} exceeds 50 μM. In the presence of low concentrations of $InsP_3$ (<5 μM), however, the two isoforms have fundamentally distinct responses to cytoplasmic $[Ca^{2+}]$ greater than 250 nM (Fig. 3). If type III $InsP_3R$ does not show Ca^{2+}-dependent inhibition, what closes the channel? The primary level of regulation may be the control of $InsP_3$ generation and degradation because type III, like type I, $InsP_3R$ only opens when $InsP_3$ is present. Further regulation of intracellular Ca^{2+} release by type III $InsP_3R$ can occur by locally depleting the intracellular Ca^{2+} stores. Other mechanisms shown to be important for type I $InsP_3R$, such as phosphorylation and regulation by associated proteins[26], may also modulate the activity of type III $InsP_3R$.

Multiple isoforms of the $InsP_3R$ are expressed in a variety of cell types[14], but the physiological significance of this was unclear. The functional differences between type I and type III isoforms of the $InsP_3R$ now indicate that each has a special role in the cell. Type I $InsP_3R$, with both Ca^{2+}-dependent activation and inhibition, is well suited for establishing Ca^{2+} oscillations[16,21,27], where the frequency of Ca^{2+} transients can be modulated when $InsP_3$ concentrations are increased[17,27]. In contrast, type III $InsP_3R$, by remaining open in the presence of high $[Ca^{2+}]$ (Fig. 3), initiates a rapid, large, and almost total release of Ca^{2+} from intracellular stores as

long as $InsP_3$ is present (Fig. 4a, d). Thus, type III $InsP_3R$ alone will not support a regenerative response, but its properties make it well suited to initiate intracellular Ca^{2+} signals. In support of this, type III $InsP_3R$ has been localized to the apical region of epithelial cells, the trigger zone from which intracellular Ca^{2+} waves originate[9–11]. Thus, the single-channel properties of type III $InsP_3R$ are well adapted to its role as the starting gate for Ca^{2+} signals in the cell.

Methods

Western blots and immunocytochemistry

Immunoblots were probed with antibodies against type I (C-19; custom produced by Research Genetics) or type III (Transduction Lab) $InsP_3R$. Blots were visualized using ECL (Kirkegaard & Perry). For immunocytochemistry, the same primary antibodies were used to probe for type I and type III $InsP_3R$ in fixed cells. The secondary antibody contained a fluorescent label (FITC) that was observed by confocal microscopy. Nonspecific staining was determined by using only the secondary antibody.

Single-channel recordings

Endoplasmic reticulum vesicles from RIN-5F cells were prepared using the protocol for cerebellum described previously[7]. Vesicles were fused into planar lipid bilayers composed of phosphatidylethanolamine and phosphatidylserine (3:1, w/w; Avanti Polar Lipids) so that the *cis* and *trans* chambers corresponded to the cytosol and lumen of the endoplasmic reticulum respectively. Cytoplasmic bilayer solutions contained 110 mM Tris and 250 mM HEPES (pH 7.35), and lumenal solutions contained 55 mM $Ba(OH_2)$ and 250 mM HEPES (pH 7.35). The *trans* chamber was held at virtual ground and the transmembrane voltage was maintained at 0 mV. Single-channel currents were recorded under voltage-clamp conditions using a patch-clamp amplifier (BC-525B, Warner Instruments) and stored on VHS tape (Instrutech). Data were filtered at 1 kHz and digitized at 4 kHz for computer analysis using pClamp 6.0.3 (Axon Instruments). For the *I–V* curve, the membrane potential was clamped at values between 5 and −30 mV. The amplitude of channel openings at each voltage was determined by fitting the data (100–1,600 openings) with a gaussian function. Single-channel conductance was determined by linear regression. An extrapolation to 0 pA to estimate the reversal potential is not included because barium (55 mM $Ba(OH)_2$) was in the *trans* chamber only, and current through the $InsP_3$-gated channel can only flow in one direction from *trans* to *cis*. Current in the opposite direction was not detected. If more positive voltages were included, the current–voltage relationship would begin to curve, and the slope conductance would be underestimated. These are the same experimental conditions as used previously for type I $InsP_3R$ (ref. 7). For the Ca^{2+} dependence curve, calibrated amounts of $CaCl_2$ were added to the cytoplasmic solution to obtain the desired free Ca^{2+} concentration. We estimated the number of active channels in each bilayer using a statistical model that is dependent on the maximum number of channels observed simultaneously, and then calculated the open probability for a single channel using this value[7,17]. Open probability data for type I $InsP_3R$ were fitted using the '2-$InsP_3$/2-Ca^{2+}' model[17], whereas open probability data for type III $InsP_3R$ were fitted according to Michaelis–Menten kinetics with $K_m = 0.3$ and $P_{max} = 5.4$: $P_o = (P_{max} \cdot [Ca^{2+}])/(K_m + [Ca^{2+}])$.

Cytoplasmic Ca^{2+} measurements

Cytoplasmic Ca^{2+} was measured in single RIN-5F cells or rat hepatocytes using confocal line scanning microscopy28 or in cell populations using ratio spectrofluorimetry29. For single-cell studies, RIN-5F cells or hepatocytes[30] were plated onto glass coverslips, incubated at 37 °C, and loaded with Fluo-3/AM (6 μM). Coverslips containing the cells were transferred to a perfusion chamber on the stage of a BioRad MRC-600 confocal microscope and observed using a 20× objective[30]. Increases in $[Ca^{2+}]$ are expressed as a percentage of baseline fluorescence[30]. Cells were examined first under control conditions, then in the presence of 0.1–

100 μM ATP. In selected experiments, RIN-5F cells were stimulated with ATP in Ca^{2+}-free medium containing 1 mM EGTA; similar results were obtained in the presence and absence of extracellular Ca^{2+}. For population studies, cells were loaded with Fura-2/AM (10 μM), then maintained at 37 °C in a cuvette. Cells were excited at 340 and 370 nm; fluorescence emission was detected at 485 nm using a PTI DeltaRAM system (these excitation and emission wavelengths were chosen to optimize Fura-2 ratio measurements with this system). Ratios were determined after background subtraction[29].

Subcellular Ca^{2+} release

RIN-5F or SKHep1 cells were placed in a perfusion chamber on the stage of a BioRad confocal microscope, then individual cells were pressure-microinjected with a solution containing 1 mM caged $InsP_3$, 1 mM Fluo-3, 1 mM HEPES, and 150 mM KCl. Cells were given 5–10 min to recover from injection, then $InsP_3$ was photoreleased using a custom-built system that couples a mercury lamp to a 1-mm quartz fibreoptic cable through a high-speed shutter and filterwheel while cells were observed using confocal line scanning microscopy[28]. SKHep1 cells were kindly provided by D. Spray.

Acknowledgments

We thank E. Kaftan for all his assistance during the execution of these experiments, J. Putney for suggesting RIN-5F cells as source of type III $InsP_3R$, and J. Brown for comments on the manuscript. This work was supported by NIH grants (to B.E.E. and M.H.N.), an Established Investigator Grant from the American Heart Association (to M.H.N.), and by the Yale Liver Center.

References

1. Furuichi T, et al. Primary structure and functional expression of the inositol 1,4,5-trisphosphate-binding protein P_{400}. Nature 1989;342:32–38. [PubMed: 2554142]
2. Mignery G, Sudhof TC, Takei K, De Camilli P. Putative receptor for inositol 1,4,5-trisphosphate similar to ryanodine receptor. Nature 1989;342:192–195. [PubMed: 2554146]
3. Sudhof TC, Newton CL, Archer BT, Ushkaryov YA, Mignery GA. Structure of a novel $InsP_3$ receptor. EMBO J 1991;10:3199–3206. [PubMed: 1655411]
4. Blondel O, Takeda J, Janssen H, Seino S, Bell GI. Sequence and functional characterization of a third inositol trisphospate receptor subtype, IP_3R-3, expressed in pancreatic islets, gastrointestinal tract, and other tissues. J Biol Chem 1993;268:11356–11363. [PubMed: 8388391]
5. Maranto AR. Primary structure, ligand binding, and localization of the human type 3 inositol 1,4,5-trisphosphate receptor expressed in intestinal epithelium. J Biol Chem 1994;269:1222–1230. [PubMed: 8288584]
6. Morgan JM, De Smedt H, Gillespie JI. Identification of three isoforms of the $InsP_3$ receptor in human myometrial smooth muscle. Pflugers Arch 1996;431:697–705. [PubMed: 8596719]
7. Bezprozvanny I, Ehrlich B. Inositol (1,4,5)-trisphosphate gated Ca channels from canine cerebellum: divalent cation conduction properties and regulation by intraluminal Ca. J Gen Physiol 1994;104:821–856. [PubMed: 7876825]
8. Perez PJ, Ramos-Franco J, Fill M, Mignery GA. Identification and functional reconstitution of the type 2 inositol 1,4,5-trisphosphate receptor from ventricular cardiac myocytes. J Biol Chem 1997;272:23961–23969. [PubMed: 9295347]
9. Nathanson MH, Fallon MB, Padfield PJ, Maranto AR. Localization of the type 3 inositol 1,4,5-trisphosphate receptor in the Ca^{2+} wave trigger zone of pancreatic acinar cells. J Biol Chem 1994;269:4693–4696. [PubMed: 7508924]
10. Thorn P, Lawrie A, Smith P, Gallacher D, Petersen OH. Local and global cytosolic Ca^{2+} oscillations in exocrine cells evoked by agonists and inositol trisphosphate. Cell 1993;74:661–668. [PubMed: 8395347]
11. Kasai H, Li Y, Miyashita Y. Subcellular distribution of Ca^{2+} release channels underlying Ca^{2+} waves and oscillations in exocrine pancrease. Cell 1993;74:669–677. [PubMed: 8395348]

12. Yoneshima H, Miyawaki A, Takayuki M, Teiichi F, Mikoshiba K. Ca^{2+} differentially regulates the ligand-affinity states of the type 1 and type 3 inositol 1,4,5-trisphosphate receptors. Biochem J 1997;322:591–596. [PubMed: 9065781]
13. Cardy TJA, Traynor D, Taylor CW. Differential regulation of types-1 and -3 inositol trisphosphate receptors by cytosolic Ca^{2+} Biochem J 1997;328:785–793. [PubMed: 9396721]
14. Wojcikiewicz RJH. Type I,II,III inositol 1,4,5-trisphosphate receptors are unequally susceptible to down-regulation and are expressed in markedly different proportions in different cell types. J Biol Chem 1995;270:11678–11683. [PubMed: 7744807]
15. DeLisle S, et al. Expression of inositol 1,4,5-trisphosphate receptors changes the Ca signal in *Xenopus* oocytes. Am J Physiol 1996;270:C1255–C1261. [PubMed: 8928753]
16. Bezprozvanny I, Watras J, Ehrlich BE. Bell-shaped calcium-response curves of $Ins(1,4,5)P_3$- and calcium-gated channels from endoplasmic reticulum of cerebellum. Nature 1991;351:751–754. [PubMed: 1648178]
17. Kaftan EJ, Ehrlich BE, Watras J. Inositol 1,4,5-trisphosphate ($InsP_3$) and calcium interact to increase the dynamic range of $InsP_3$ receptor-dependent calcium signaling. J Gen Physiol 1997;110:529–538. [PubMed: 9348325]
18. Thomas AP, Bird GS, Hajinoczky G, Robb-Gaspers LD, Putney JW. Spatial and temporal aspects of cellular calcium signaling. FASEB J 1996;10:1505–1517. [PubMed: 8940296]
19. Dubyak GR, El-Moatassim C. Signal transduction via P2-purinergic receptors for extracellular ATP and other nucleotides. Am J Physiol Cell Physiol 1993;265:C577–C606.
20. Cao D, Lin G, Westphale E, Beyer E, Steinberg T. Mechanisms for the coordination of intercellular calcium signaling in insulin-secreting cells. J Cell Sci 1997;110:497–504. [PubMed: 9067601]
21. Dixon C, Woods N, Cuthbertson K, Cobbold P. Evidence for two Ca2(+)-mobilizing purinoceptors on rat hepatocytes. Biochem J 1990;269:499–502. [PubMed: 2386488]
22. Bootman M, Berridge M, Lipp P. Cooking with calcium: the recipes for composing global signals from elementary events. Cell 1997;91:367–373. [PubMed: 9363945]
23. Parker I, Yao Y. Ca^{2+} transients associated with openings of inositol trisphosphate-gated channels in *Xenopus* oocytes. J Physiol 1996;49:663–668. [PubMed: 8815201]
24. Lipp P, Thomas D, Berridge M, Bootman M. Nuclear calcium signalling by individual cytoplasmic calcium puffs. EMBO J 1997;16:7166–7173. [PubMed: 9384593]
25. Glennon MC, Bird GSJ, Kwan CY, Putney JW. Actions of vasopressin and the Ca^{2+}-ATPase inhibitor, thapsigargin, on Ca^{2+} signaling in hepatocytes. J Biol Chem 1992;267:8230–8233. [PubMed: 1533221]
26. Cameron A, et al. Calcineurin associated with the inositol 1,4,5-trisphosphate receptor–FKBP12 complex modulates Ca^{2+} flux. Cell 1995;83:463–472. [PubMed: 8521476]
27. Petersen CC, Toescu EC, Potter BVL, Petersen OH. Inositol triphosphate produces different patterns of cytoplasmic Ca^{2+} spiking depending on its concentration. FEBS Lett 1991;293:179–182. [PubMed: 1959657]
28. Nathanson MH, Padfield PJ, O'Sullivan AJ, Burgstahler AD, Jamieson JD. Mechanism of Ca^{2+} wave propagation in pancreatic acinar cells. J Biol Chem 1992;267:18118–18121. [PubMed: 1517244]
29. Grynkiewicz G, Poenie M, Tsien R. A new generation of Ca^{2+} indicators with greatly improved fluorescence properties. J Biol Chem 1985;260:3440–3450. [PubMed: 3838314]
30. Schlosser SF, Burgstahler AD, Nathanson MH. Isolated rat hepatocytes can signal to other hepatocytes and bile duct cells by release of nucleotides. Proc Natl Acad Sci USA 1996;93:9948–9953. [PubMed: 8790437]

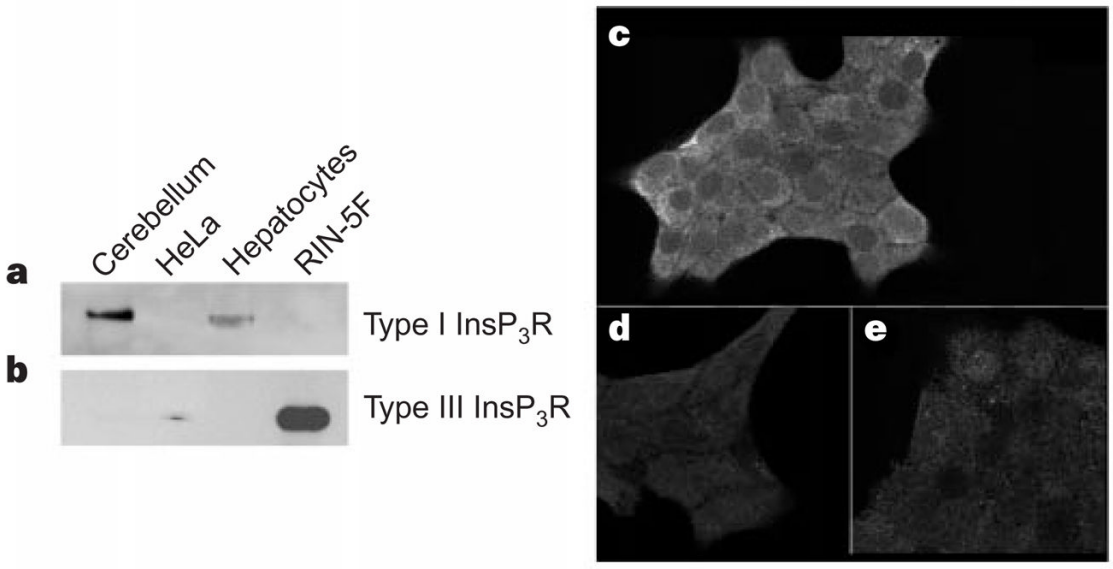

Figure 1.

RIN-5F cells preferentially express Type III $InsP_3R$. **a**, **b**, Western blots were probed for types I and III $InsP_3R$ (**a** and **b**, respectively). Dog cerebellum and rat hepatocytes were positive controls for type I $InsP_3R$; HeLa cells were a positive control for type III $InsP_3R$. Lanes were loaded with 30 μg dog cerebellar microsomes (lane 1), 10 μg HeLa cell lysate (lane 2), 30 μg hepatic microsomes (lane 3), and either 30 μg (**a**) or 5 μg (**b**) of RIN-5F microsomes (lane 4). **c**, **e**, Cellular distribution of type III (**c**) and type I (**e**) $InsP_3R$ in RIN-5F cells. **d**, Nonspecific binding.

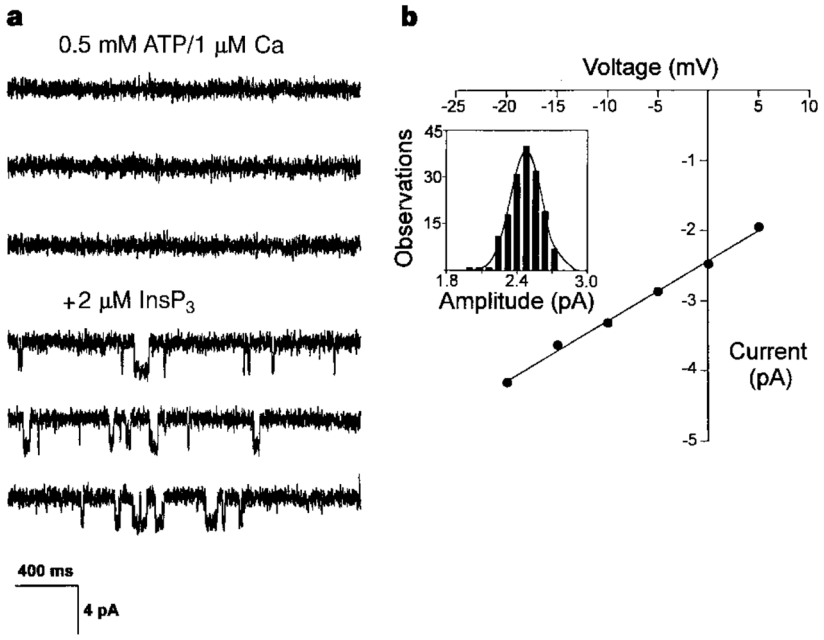

Figure 2.

Type III $InsP_3R$ is an $InsP_3$-gated Ca^{2+} channel. **a**, $InsP_3$-gated Ca^{2+} channels from endoplasmic reticulum of RIN-5F cells in planar lipid bilayers. In the absence of $InsP_3$, channel activity was not observed (top three traces). Addition of 2 μM $InsP_3$ to the cytoplasmic side induced channel activity (bottom three traces). Channel openings are shown as downward deflections from baseline. Ruthenium red (2 μM) was present to block ryanodine receptors. **b**, Current–voltage relationship of type III $InsP_3R$. Inset shows an amplitude histogram at 0 mV for one experiment. Values plotted in the *I–V* curve represent the mean for three experiments. Standard errors for data points, which range from 0.02 to 0.05 pA, are too small to be seen.

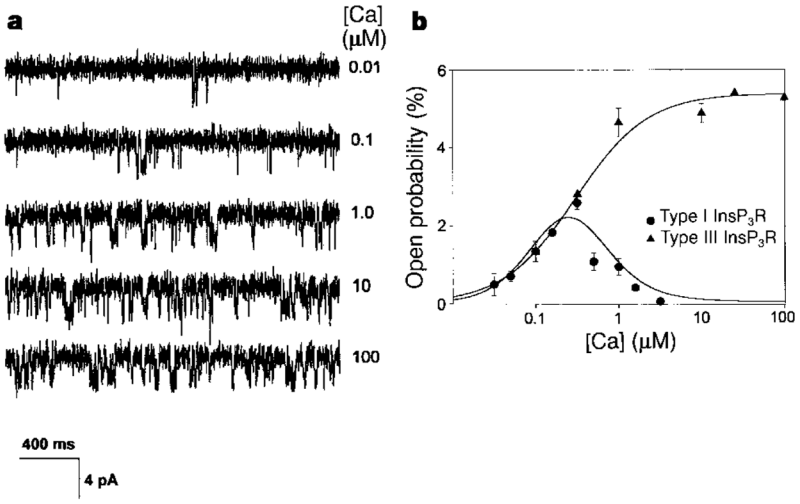

Figure 3.

Single channel open probability for type I and type III $InsP_3R$ as a function of Ca^{2+} concentration. **a**, Channel activity for type III $InsP_3R$ in the presence of 2 μM $InsP_3$, 0.5 mM ATP, 0.5 mM EGTA, 2 μM ruthenium red, and at 0 mV. Channel openings are shown as downward deflections. **b**, Single channel open probability of type I $InsP_3R$ (circles) and type III $InsP_3R$ (triangles). Data points for type I $InsP_3R$ were taken from ref.[17]. Data for three experiments are shown for type III $InsP_3R$. Individual points with error bars are the mean ± s.e.m. for $n = 2$ (1 and 10 μM Ca^{2+}) or $n = 3$ (0.01 and 0.1 μM Ca^{2+}).

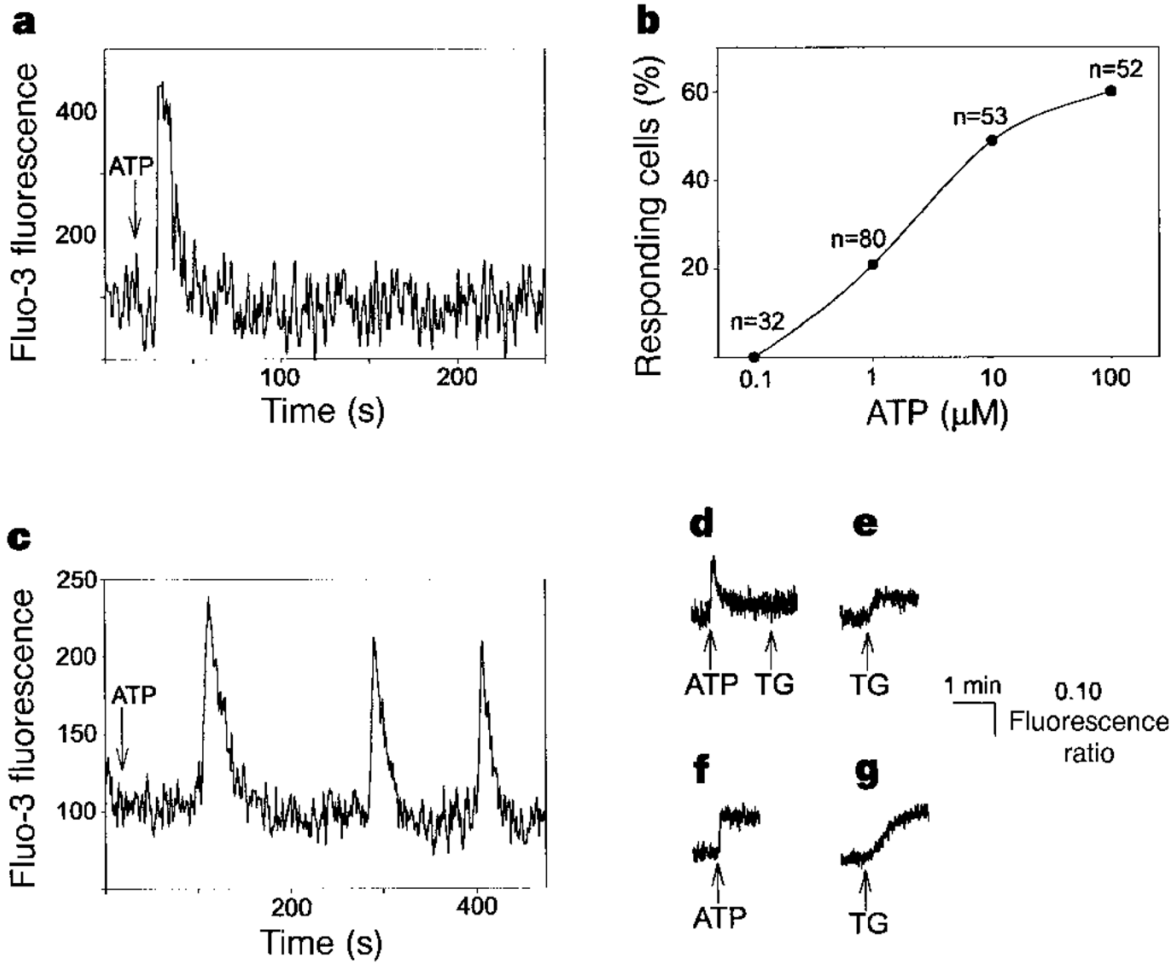

Figure 4.

Ca^{2+} signalling patterns in RIN-5F cells and rat hepatocytes. **a**, Stimulation of a RIN-5F cell with 100 μM ATP induces a single intracellular Ca^{2+} transient. **b**, Dose–response curve for RIN-5F cells stimulated with ATP. Values indicate total numbers of cells stimulated. **c**, Stimulation of an hepatocyte with 1 μM ATP induces Ca^{2+} oscillations. **d**, ATP (100 μM) induces a single transient increase in Ca^{2+} in RIN-5F populations (peak change in fluorescence ratio, $\Delta R = 0.20 \pm 0.01$; $n = 6$). Subsequent treatment with thapsigargin (TG; 2 μM) has little effect on Ca^{2+} ($\Delta R = 0.03 \pm 0.01$; $n = 6$). **e**, Thapsigargin alone (2 μM) increases Ca^{2+} in RIN-5F cells ($\Delta R = 0.08 \pm 0.01$; $n = 6$). **f**, ATP (100 μM) induces a rapid, sustained increase in Ca^{2+} in hepatocyte populations ($\Delta R = 0.13 \pm 0.02$; $n = 7$). **g**, Thapsigargin (2 μM) increases Ca^{2+} in hepatocytes like ATP alone ($\Delta R = 0.10 \pm 0.02$; $n = 7$).

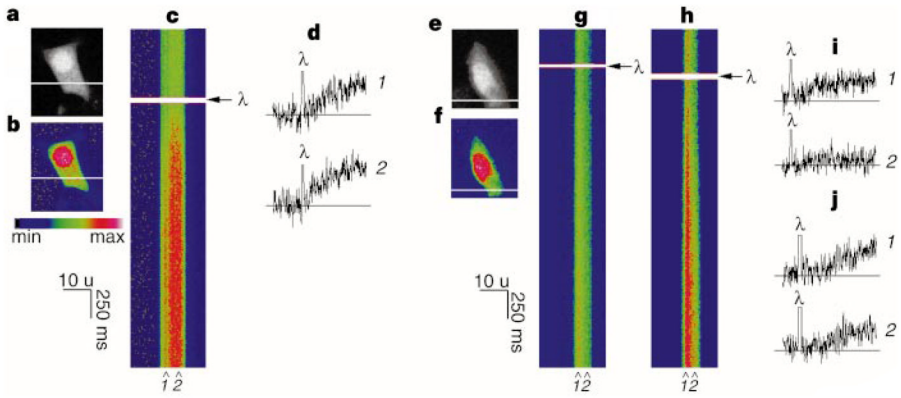

Figure 5.

Subcellular Ca^{2+} release differs between RIN-5F and SKHep1 cells. **a**, confocal image of a RIN-5F cell. **b**, Pseudocolour image of the cell loaded with Fluo-3. The same pseudocolour scale was used for **b**, **c**, and **f**–**h. c**, Line scan collected along the line indicated in **b** after flash photolysis (λ) of caged $InsP_3$. Ca^{2+} increases throughout the cell after photorelease of $InsP_3$ (representative of 13 experiments with flash duration 50–100 ms). No Ca^{2+} increase was detected in 6 experiments with flash duration <50 ms. Spatial resolution, 0.26 μm per pixel; temporal resolution, 6 ms per pixel. **d**, Release of caged $InsP_3$ results in a global increase in Ca^{2+}. Trace duration in **d**, **i** and **j** is 2 s. **e**, **f**, Confocal (**e**) and pseudocolour (**f**) images of an SKHep1 cell. **g**, **h**, Confocal line scans of the cell during 30 and 60 ms flashes to photolyse caged $InsP_3$. A response is detected in only the left side of the cell after a short flash (**g**), and throughout the cell after a long flash (**h**). Responses were absent or minimal in only part of an SKHep1 cell in 7 experiments (flash duration, 3–50 ms), whereas global Ca^{2+} increases were seen in 12 experiments (flash duration, 5–60 ms). **i**, An increase occurs on the left side of the cell in **g** (1), but not on the right (2). **j**, After more photorelease of $InsP_3$ (**h**), similar Ca^{2+} increases occur at the same two subcellular locations.

Table 1

Ca^{2+} transients in RIN-5F cells after stimulation by ATP

ATP (μM)	Magnitude (% increase)	Duration (s)
100	209 ± 24 (*n* = 23)	15.2 ± 0.8 (*n* = 31)
100 (Ca^{2+}-free)	200 ± 13 (*n* = 25)	14.8 ± 1.2 (*n* = 25)
10	160 ± 14 (*n* = 25)	16.8 ± 2.1 (*n* = 19)
1	121 ± 15 (*n* = 15)	13.0 ± 2.1 (*n* = 8)
0.1	0 (*n* = 32)	0 (*n* = 32)

RIN-5F cells were stimulated with ATP and changes in cytoplasmic Ca^{2+} in individual cells were measured by Fluo-3 fluorescence using confocal line scanning microscopy. The magnitude (per cent increase over baseline) and duration of the Ca^{2+} transients are expressed as mean ± s.e.m. (*n*).